

# On final states of 2D decaying turbulence

Z. Yin<sup>1</sup>

Fluid Dynamics Laboratory, Applied Physics Department, Eindhoven  
University of Technology, P.O.Box 513, 5600 MB, Eindhoven, The  
Netherlands

LSEC, Institute of Computational Mathematics, Chinese Academy of  
Sciences, P.O.Box 2719, Beijing 100080 P.R.China

Numerical and analytical studies of “final states” of two-dimensional (2D) decaying turbulence are reported. The first part of this work is trying to give a definition for final states of 2D decaying turbulence. Although the functional relation of  $\omega - \psi$  is frequently used as the characterization of those “final states,” it is just a sufficient but not necessary condition so it is not proper to be used as the definition. It is found the way through the value of the effective area  $S$  covered by the scatter  $\omega - \psi$  plot, which is initially suggested by Read [1], is more general, and more suitable for the definition. Based on this concept, we gave out a definition that can cover all existing results in late states of decaying 2D flows, including some weird double-valued  $\omega - \psi$  scatter plots that can not be explained before. The rest part of the paper is trying to further investigate 2D decaying turbulence with the assistance of our new definition. Some new numerical results, which lead to “bar” final states and further verify the predictive ability of statistical mechanics [2], are reported. It is realized that some simulations with narrow-band energy spectral initial conditions, which can be called “turbulence” doubtfully, lead to some final states that can not be very well explained by the statistical theory (in the meanwhile, they are still in the scope of our new definition of the “final state”). For those simulations with initial conditions of broadband energy spectra that lead to the famous dipole, we give out a mathematical re-interpreting for the so-called sin-hyperbolic (“sinh”)  $\omega - \psi$  scatter plot in final states. We suggest the term “sinh” here should be replaced by “sinh-like.” The corresponding physical meaning of this re-interpreting will also be discussed.

## I. INTRODUCTION

It is an interesting topic to study final states of two-dimensional decaying turbulence. Recent publications [2] (hereafter YMC) and [3] show that nu-

---

<sup>1</sup>Electronic address: yinzh@lsec.cc.ac.cn

merical simulations starting from different initial conditions (depending on the size of patches in the vorticity field) can lead to different final states. The statistical mechanics in two-dimensional turbulence, known as the “point” theory and the “patch” theory, shows a great predictive power in this kind of simulations.

The “point” theory is concerned with a mean-field treatment of ideal line vortices, which had been given thirty years ago [4, 5]. The system is Hamiltonian with a finite phase space, applied by Boltzmann statistics to its dynamics initially by Onsager [6]. It was further developed by several groups [7-23]. In these investigations, it is surprise to see that the ideal Euler mean-field predictions fit the Navier-Stokes results.

The “patch” theory started from the late 1980s [24-29]. In the “patch” theory, the delta-functions that are used to discretize the vorticity field in the “point” theory are replaced by finite-area, mutually exclusive “patches” of vorticity. The Lynden-Bell statistics [30] is applied to this theory.

The predictive abilities of these two theories are tested after defining the related entropy of them and developing the precise formulas suited for calculations, the details of which are given in *Spring Notes* by D.C. Montgomery (private communication; see also a modified version of it in chapter 2 of [31]). Several kinds of solutions in the double periodical domain from the statistical mechanics are considered. It is found that the traditional “dipole” or the one-dimensional “bar” solution will have the largest entropy under different conditions: for the vorticity field with large patch vortices, the “bar” solution is the maximum entropy state, and the “dipole” will dominate the final state if only point vortices or small patches exist initially. The prediction is validated by most of our direct numerical simulations, which are well represented by 13 simulations listed in [31]. These simulations, which make use of Fourier pseudo-spectral methods, have considerable high resolutions ( $512^2$ ) and have been run long enough (100 - 1500 turnover times) to make sure to reach final states. Those runs tested theoretical results through all kinds of aspects: from maximum entropy states to local maximum states. We even found a couple of results that lead to unclassified states, which are excluded by the most general case of the “patch” theory (see section II and III for some of them).

However, comparing to considerable efforts to investigate the “final state” of 2D turbulence, few efforts have been devoted to define it. There exist some characters when the term of “final states” in 2D flows is referred to, but they are rather blurred and it is very easy to find some negative examples for them as the investigation in this field goes on.

For example, sometimes it is thought that the flow field has reached the

“final state” if the pattern of the flow remains unchanged for a certain long time. However, in our sinh-Poisson quadrupole to “dipole” simulation (Figs. 7 in [3]), the quadrupole in the vorticity field lasts so long (from  $t \cong 0$  to  $t \cong 150$ ) that people might think the “final state” has already been reached, while the continued calculation showed that it is just a local maximum state.

There are still some other characters except the example above (we will discuss another one in detail later in section IIA). Those characters are important phenomena of “final states.” In the meanwhile, they can be very misleading. Thus it is necessary to give out a definition which can include all exiting cases of “final states.”

This definition will play an important role when a long direct numerical simulation of decaying turbulence is carried out. It can be used to decide when the code should be stopped. This is not a trivial decision since some of the results (including the “bar” final state) in YMC are obtained partly because of the continuing calculation after former researchers stopped [32] (of course, those runs are mainly stimulated by theoretical results of the statistical-mechanics). In our former investigation, the pseudo-spectral code has been continued as long as possible to make sure that final states have been reached. The calculation can be significantly extended without a good definition of the “final state.” On the other hand, because of the existing bottleneck in parallelization of the 2D pseudo-spectral code [3], the extended calculation might mean several extra weeks (the wall clock time) for runs with the resolution of  $512^2$ . The future investigation in this field may involve in simulations with the resolutions of  $1024^2$  or higher. For those high-resolution simulations, even with the fastest parallel spectral Fourier 2D code we have so far (using the combined technique of domain decomposition and task distribution [33]), it would be a nightmare for the investigation if no clue is used to judge the final state and a lot of extended computation is needed to make sure that there is no interesting new phenomenon any more. In section II, we will try to give out a definition of “final states” for those kinds of purposes.

In section III, with the assistance of the new definition of “final states,” (on the other hand, in order to validate the definition), some numerical simulations are carried out. This part of the work can be also treated as the continued investigation of YMC. Former numerical results in YMC leading to “bar” final states are confined by an initial symmetric quadrupole with a certain amount of noise added to break the symmetry and accelerate the process of computations. Without further proofs, it can be argued that the “bar” is reached only because of the existing symmetry in the main structure. Hence the generality of this kind of solutions might be endangered. In section

III, some other techniques are adopted to break the symmetry, and again they end up with “bar” states. These simulations also confirm our former statement (in a much more direct sense): “it is the size of the ‘patch’ that plays a key role in the process towards the ‘bar’ final state.”

In section IIIB, another totally different initial condition leading to the “bar” will be reported. Although the statistical mechanics can predict the flow pattern for the final state of that simulation (the patch size in the initial vorticity field is big, and thus the “bar” is expected [2]), it has some difficulties when explaining the  $\omega - \psi$  scatter plot at the late time. Here, it should be noticed that that “final state” is still in the scope of our new definition in section IIB.

Section IV is concerned with an influential simulation in this field [34-36]. The question was raised when we tried to repeat the pioneers’ work - changing the parameters of the sin-hyperbolic (sinh) function to make a best fit for the scatter  $\omega - \psi$  plot of the famous “dipole.” This fitting process gave us the hallucination that the sum of several sinh functions is just another sinh function. Of course, this is wrong, and the fitting error can be reduced dramatically by using the combination of several instead of just one sinh function. The corresponding physical meaning of this fitting process will also be discussed. The main content of this section is more concerned with the conception of the statistical mechanics than presenting new results: it is suggested to replace the term “sinh” in existing literatures of this field by the term “sinh-like” to represent the “point” theory and numerical results better.

There are mainly two threads when we are writing this paper: the first one is the new definition of “final states,” another one is that this paper is the extended work of YMC.

## II. DEFINING THE “FINAL STATE” IN 2D TURBULENCE

### A. Starting from a sufficient but not necessary condition of “final states”

In 2D flow field, if we denote the vorticity as  $\omega$ , and the stream function  $\psi$ , the Navier-Stokes equation can be written as

$$\frac{\partial \omega}{\partial t} + \left( \frac{\partial \omega}{\partial x} \frac{\partial \psi}{\partial y} - \frac{\partial \omega}{\partial y} \frac{\partial \psi}{\partial x} \right) = \nu \nabla^2 \omega \quad (1)$$

and

$$\omega = -\nabla^2\psi, \quad (2)$$

with  $\nu$  the kinematic viscosity of the fluid.

A shorthand notation for the nonlinear contribution to Eq. (1) is the Jacobian  $J(\omega, \psi)$

$$J(\omega, \psi) = \frac{\partial\omega}{\partial x} \frac{\partial\psi}{\partial y} - \frac{\partial\omega}{\partial y} \frac{\partial\psi}{\partial x}. \quad (3)$$

For inviscid flows, Eq. (1) reduces to the Euler equation

$$\frac{D\omega}{Dt} = \frac{\partial\omega}{\partial t} + J(\omega, \psi) = 0, \quad (4)$$

which states that the vorticity of a fluid element is conserved for inviscid flows (note that  $D\omega/Dt$  represents the material derivative).

It can be seen that if there exists a functional relation  $\omega = f(\psi)$ , then

$$J(\omega, \psi) = \frac{\partial f(\psi)}{\partial x} \frac{\partial\psi}{\partial y} - \frac{\partial f(\psi)}{\partial y} \frac{\partial\psi}{\partial x} = \left(\frac{\partial f}{\partial\psi} \frac{\partial\psi}{\partial x}\right) \frac{\partial\psi}{\partial y} - \left(\frac{\partial f}{\partial\psi} \frac{\partial\psi}{\partial y}\right) \frac{\partial\psi}{\partial x} = 0. \quad (5)$$

This means that the experimental or numerical observation of the functional relationship  $\omega = f(\psi)$  indicates the presence of a stationary state of inviscid flow. Usually, this observation is treated as an indication of the presence of a nearly steady state of high Reynolds number flows, *i.e.*, the case when  $\nu \rightarrow 0$ .

*Although the  $\omega - \psi$  functional relation is an important tool in the characterization of so-called “final states” of decaying 2D turbulence, we should notice that it is a sufficient but not necessary condition of near-equilibrium states of high Reynolds number flows.*

In Figs. 1, we see a good example of the functional relationship between  $\omega$  and  $\psi$  - the famous Lamb dipole (for further details see [37, 38]). It has the linear relation of  $\omega - \psi$  (for  $-0.5 < \psi < 0.5$ ). Another example is the sinh relationship [34-36], of which we will give a re-interpreting as the “sinh-like” relation in section IV.

In Figs. 2, we see a double-valued structure of the  $\omega - \psi$  plot [39] and the associated  $\omega$  and  $\psi$  contour plots. They come from one simulation in YMC - Figs. 18 and 19, which cannot be explained by the existing statistical-mechanical theories. By comparing the  $\omega - \psi$  scatter plot with the contour plots of the vorticity and the stream function, we can conclude that the larger negative vortex, which is indicated by the solid arrow, corresponds to

the longer negative branch of the  $\omega - \psi$  scatter plot. In the meanwhile, the shorter (negative) branch of the  $\omega - \psi$  scatter plot represents the smaller negative vortex (see the dashed arrow).

The vorticity field shown in Fig. 2(a) represents a stationary solution of the Euler equation  $D\omega/Dt = 0$ . This can be demonstrated numerically: what we did is using the pseudo-spectral Fourier code of the Navier-Stokes equation and setting  $\nu = 0$  (this is the handiest way to test it in our case); the exact vorticity field of Fig. 2(a) (without any noise) is used as the initial condition for a simulation with the resolution of  $512^2$ . The simulation lasts for  $3 \times 10^5$  time steps (the time step is  $1/2000$ ), which is about 400 turnover times if we set  $\nu = 1/5000$ . However, the vorticity field has not been changed a bit from  $t = 0$  to  $t = 150$ . The continuing running of the code is more a test of the accuracy of the pseudo-spectral method than anything else.

This double-valued structure cannot be explained by the statistical-mechanical theory for Euler flows, even if the most general formulation of the “patch” theory

$$\nabla^2\psi = -\omega = -\sum_{j=1}^q \frac{M}{\Delta} K_j \frac{e^{\alpha_j - \beta\psi K_j}}{\sum_{l=0}^q e^{\alpha_l - \beta\psi K_l}} \quad (6)$$

is taken into consideration.

At this point, we should admit that although the application of a statistical-mechanical approach to predict the quasi-stationary final state of inviscid flows appears to be very powerful to investigate freely evolving 2D turbulent flows, it still has some limitations, which cannot be easily understood.

The flow is not described by any functional relation between  $\omega$  and  $\psi$ , but it manages to go to one specific kind of equilibrium states. This is partly due to the fact that this simulation starts from a condition with narrow-band energy spectra - more specifically, most of the energy is concentrated in few low wave numbers. Because of inverse energy cascade phenomena in 2D turbulence (the energy is mainly transferred to lower wave numbers), the state of broad-band energy spectra, where the statistical mechanics might take effect, can never be reached.

Anyway, the functional relation of  $\omega - \psi$  is not enough to define the “final state,” we need something else to be used as the definition. And this will be the main task in the following subsection.

## B. A definition covering all existing possibilities

To estimate the quantitative flux across the region, people normally use a diagnostic technique first described by Read *et al.* [1]. They showed that the net flux of vorticity out of a closed loop in the physical space is equal to the effective area enclosed by the corresponding circuit in the  $\omega - \psi$  space. However, the usage of the effective area so far is limited to indicate how far away from the state of the  $\omega - \psi$  functional relation the flow field is [40, 41]. In the following, we will show that it is in fact a more powerful and more general judgment for equilibrium states of 2D turbulence than the simple  $\omega - \psi$  functional relation.

For the integrality of this paper, this judgment will be re-stated as follows:

- At a certain stage of a numerical simulation of 2D decaying turbulence, draw a closed circuit in the contour plot of  $\psi$  that can represent the whole flow field, find enough points on this circuit and mark them in order. In Fig. 3(a), we only use 5 points for convenience.
- Find the corresponding points in the scatter plot of  $\omega - \psi$  at the same time of the simulation. There will be two kinds of possibilities:
  1. Those points form a simple circuit, the area of which is equal to the effective area  $S$  (Fig. 3(b)).
  2. Those points form a region that is reentrant. The effective area  $S$  in this case is equal to the sum of anticlockwise areas minus the sum of clockwise areas. For example, in Fig. 3(c), the effective area  $S$  is

$$S = S_{anticlockwise} - S_{clockwise} = S_1 - S_2. \quad (7)$$

(In Fig. 3(c), we only draw one clockwise and one anticlockwise region for convenience. In a real problem, it may have several clockwise and anticlockwise areas respectively.)

- The absolute value of  $S$  indicates how far away the flow field is from the equilibrium state. The larger the absolute value of  $S$ , the further away the flow field from the final state. On the other hand, if the absolute value of  $S$  is very small ( $S \cong 0$ ), it means that the equilibrium state has been reached.

- The condition of  $S \cong 0$  is only enough to judge the equilibrium state of 2D turbulence. To define the “final state,” it is necessary to remove those local maximum states (see for examples in section IIIB2 of YMC).

To sum up, the “final state” of 2D turbulence can be defined as:

*The flow field of 2D turbulence has reached the “final state” if the following two conditions are true:*

- *The effective area  $S \cong 0$ ;*
- *It is not a local maximum state.*

Note that the “real” final state of the flow field is the zero vorticity state ( $\omega \equiv 0$ ) when the decaying process really stops. But those cases are not interesting to us. The “final state” that we are talking about is actually a stage when the continuing numerical simulation will not lead to any new interesting phenomenon.

Here, the condition of  $S \cong 0$  cannot be strictly defined. How small the absolute value of  $S$  should be depends on different specific conditions. According to our experience, it is more useful to look into the scatter plot of  $\omega - \psi$  itself than to give out any specific value.

In the following, we will use the new definition to analyze different situations:

- For those results with the functional relation of  $\omega - \psi$  such as the lamb dipole or the “sinh-like” relation discussed in the previous subsection, it is obvious that  $S \cong 0$  - the “final state” has been reached.
- For those results with multi-valued structures in  $\omega - \psi$  plots, there are three kinds of situations:
  1. If that multi-valued structure does not close any area ( $S \cong 0$ ), such as Fig. 2(c), it can be also said that the final state has been reached. (Actually Fig. 2(c) is not a good example: if we put some noise onto the weird quadrupole, and use it as the initial condition of a DNS run, we will end up with a normal sense of the  $\omega - \psi$  functional relation. So actually this weird quadrupole is just a local maximum state. However, we have to make the definition be able to sort out similar situations with maximum entropies, which might appear in the future research.)



2. If that multi-valued structure does close some areas, but they are arranged clockwise and anticlockwise, and can cancel each other (again,  $S \cong 0$ ). We can also say that the “final state” has been reached. (We will show an example in section IIIB.)
3. If that multi-valued structure closes some areas, but clockwise and anticlockwise parts of them cannot cancel each other, then the final state has not been reached, and continuing calculations are needed. An extreme example is a state when the scatter points of  $\omega - \psi$  are distributed across the whole plot, which normally happens when the simulation was started using some random initial condition.

With this judgment, we can easily sort out those non-equilibrium states such as the traveling wave in the patch quadrupole to the “bar” simulation (Figs. 4).

### III. FURTHER INVESTIGATIONS ON THE “BAR” FINAL STATE

In YMC, we have investigated the emergence of the “bar” final state by considering an antisymmetric basic flow (the quadrupole solution) with a considerable amount of noise added to it in order to break the symmetry of the basic flow. We decided to devote some more efforts to find other initial conditions leading to the “bar” quasi-stationary final state, and it will be seen shortly that the appearance of the “bar” final state is not that accidental as might erroneously be concluded from the previous set of simulations.

The simulations are finished by the dynamical pseudo-spectral-code of the 2D NS equation, using a resolution of  $512 \times 512$  Fourier modes. The time step in all simulations is fixed at  $1/2000$  and determined by the CFL condition. The initial energy, using the normalization of

$$E = \frac{1}{2} \frac{1}{(2\pi)^2} \iint \omega \psi dx dy$$

is 0.5. There is no hyperviscosity or small-scale smoothing of any kind in our simulations.

#### A. Simulations by shrinking the size of “patches” in the initial field

The first idea here is to start from the same quadrupolar “patch” initial condition as YMC, but distort the initial condition slightly in the follow-

ing way: we shrink the patch size with a small amount and reposition the patches slightly (see, for example, the plots in the first row of Figs. 5). The symmetry of the basic flow has been broken already, and there is no need to add any noise to it (unlike what we did in Fig. 7(b) of YMC). The Reynolds number is fixed at  $1/\nu = 8000$ . As can be seen from Figs. 5, we have performed two simulations with two different distorted quadrupolar initial conditions, with the patch size reduced by a factor of  $7/8 \times 7/8 = 49/64$  compared to the patch size of the original quadrupole initial condition (see Fig. 7(a) in YMC), and both runs clearly reveal the emergence of the quasi-stationary “bar” final state. A similar set of simulations has been carried out, but now with the patch size even further reduced. In Figs. 6, we have shown the vorticity contour plots of runs with the patch size reduced by a factor of  $3/4 \times 3/4 = 9/16$ , and it is clear that no “bar” final state is found in this case.

We may recall that in Figs. 4 of YMC, the E-S plot predicts that for doubly-periodical domain, large “patch” vortices lead to the “bar” quasi-stationary final state and small “patch” vortices lead to the “dipole” final state. In YMC, we only test two extreme cases of theoretical results – the initial quadrupole solutions with the largest patches (Figs. 7-10 in YMC) and the smallest patches - “point” (Figs. 14-16 in YMC). There is no intermediate simulation that can make the logic more complete. The four simulations in Figs. 5,6 provide a much more direct proof for our theoretical results of the statistical-mechanics. We can predict that if the size of the patch is shrunk further (by a factor even smaller than 9/16), the numerical simulation will lead to the dipole final state.

One question that might be raised concerns the direction of the “bar” final state. As can be observed in Figs. 5, it can happen in the horizontal or vertical direction (and should occur with equal probability due to their symmetrical equivalence). However, the “bar” final state (with  $2\pi$  periodicity perpendicular to the flow direction) has never been observed in any other direction due to lack of periodicity of such a solution. Note that a solution with periodicity less than  $2\pi$  perpendicular to the flow direction enables a flow rotated with respect to the x and y direction (e.g., a direction of  $45^\circ$  is needed for a bar solution with a  $\sqrt{2}\pi$ - periodicity).

Due to the inverse energy cascade phenomenon in 2D turbulence, most of the energy will be concentrated on the lowest modes of wavenumber at final states - there are four modes altogether:

$$\vec{k} = (k_x, k_y) = (1, 0), (-1, 0), (0, 1) \text{ or } (0, -1).$$

Different combinations of these four modes dominate flow patterns at

final states. Here are three kinds of possibilities altogether:

- If energies are more or less equally distributed in these four modes, we will get the dipole (see the last vorticity contour plot in Figs. 5 of YMC);
- If energies are concentrated on either (1,0), (-1,0) or (0,1), (0, -1), then we will get “bar” final states (like Figs. 5);
- If energies are distributed on those modes unequally, then we will get a final state between “dipole” and “bar” (like Figs. 6, especially Figs. 6(b)).

## B. The “slanting bar” to “bar” simulation

We have conducted another set of simulations with initial conditions that was found to lead to the “bar” final state. The initial condition is based on the slanting bar solution already referred to in the previous subsection ( $\sqrt{2}\pi$ -periodicity), where a certain amount of noise is added to it to break the symmetry. We let the flow evolve and as shown in Figs. 7, the “bar” final solution is obtained eventually. The Reynolds number in this simulation is fixed at  $1/\nu = 8000$ . The initial Taylor-scale Reynolds number

$$R_\lambda \approx \sqrt{\frac{10}{3}} \frac{E}{v\sqrt{\Omega}} \approx 4002.$$

It increases to 8035 at the end of the simulation. Attention should be drawn to the  $\omega - \psi$  scatter plot obtained at the end of the simulation. It is similar to the scatter plot obtained for the “bar” solution in Fig. 9 of YMC, but some subtle differences can be observed. When considered in more details, the scatter plot is in fact a double-valued structure. However, this double-valued structure is different from the open line in Fig. 2(c). It is a structure that actually encloses some areas. We maybe recall the discussion in the previous section that if those areas cannot cancel each other, namely  $S \neq 0$ , it may mean that the “final state” has not been reached and the continuing calculation is needed.

However, with a close examine of the  $\omega - \psi$  scatter plot, we will find that the region covered by scatter points is actually reentrant, and thus  $S \approx 0$ :

This procedure can be done by drawing a line from the bottom to the top of the contour plot of  $\psi$  (see the arrow line at the last figure in the right column of Figs. 7). It is not necessary

to draw a loop (like what we did in Fig. 3(a)) in this case, because we are dealing with the doubly-periodical condition, and a straight line that connects two opposite boundaries is already enough to make a loop. At the late stage of this simulation, the flow field is essentially one-dimensional. It is possible to gather all the information by studying this straight line. As indicated in Fig. 8, the corresponding points in  $\omega - \psi$  plot form a clockwise region and an anticlockwise region, which can almost cancel each other (see Eq. (7)). So in fact, the absolute value of the effective area  $S$  is very small - the “final state” has been reached.

This simulation illustrates one special case that our new “final state” definition covers (see the second last paragraph in section IIB).

Again, the statistical mechanics cannot explain this double-valued structure due to the less “turbulent” initial condition.

## IV. A RE-INTERPRETING FOR THE $\omega - \psi$ PLOT OF THE FAMOUS DIPOLE

About a decade ago, Matthaeus *et al.* [34-36] reported the first long time simulation which led to the “dipole” final state. They used the sinh function to fit the scatter  $\omega - \psi$  plot at the late time [36] for the first time, and they found a close fitting function by changing the values of  $\alpha$  and  $\beta$  in

$$\omega = \alpha \sinh(\beta\psi). \quad (8)$$

However, we will argue that it is not enough to use only one single sinh function, more sinh functions should be adopted to fit the scatter plot. The first subsection will tell people a fake theorem, which is the reason why the pioneer works are restricted themselves to one sinh function. The second subsection will be our re-interpreting of the  $\omega - \psi$  plot.

### A. Starting from a fake theorem

The fake theorem states as follows:

*$\forall \alpha_1, \alpha_2, \beta_1, \beta_2 \in \text{real numbers}$ , there are two real numbers  $\alpha_0$  and  $\beta_0$ , which make the following equation true:*

$$\alpha_1 \sinh(\beta_1 x) + \alpha_2 \sinh(\beta_2 x) = \alpha_0 \sinh(\beta_0 x). \quad (9)$$

If the theorem above is true, we can easily get a more general conclusion from it:

$\forall \alpha_i, \beta_i (i = 1, 2, 3, \dots n) \in \text{real numbers}$ , there are two real numbers  $\alpha_0$  and  $\beta_0$ , which make the following equation true:

$$\sum_{i=1}^n \alpha_i \sinh(\beta_i x) = \alpha_0 \sinh(\beta_0 x). \quad (10)$$

Eqs. (9) and (10) are not reasonable at the first thought, but Figs. 9, which are the plots of the following functions, seem to cater for them:

$$y = 0.00008 \sinh(2x), \quad (11)$$

$$y = 0.05 \sum_{i=1}^{100} \sin(i) * \sinh\left(\frac{x}{i}\right), \quad (12)$$

and

$$y = 0.0001 \sum_{i=1}^{100} \sin(i) * \sinh\left(2^{\frac{1}{i}} x\right). \quad (13)$$

Figs. 9(b, c) look so much like a sinh function that they give us the feeling that we can always find a good combination of the parameters  $\alpha_0, \beta_0$ , which makes the simple sinh function ( $\alpha_0 \sinh(\beta_0 x)$ ) fit any of those figures (as what Eq. (10) indicated).

We have drawn the plot of  $y = \sum_{i=1}^n \alpha_i \sinh(\beta_i x)$  with other different values of  $n, \alpha_i$ , and  $\beta_i$ , it always looks like a single sinh function.

Of course, Eqs. (9) and (10) are not true. They can be easily disproved after comparing the first few coefficients of the Taylor series in both sides of the equal mark.

## B. “Sinh” or “sinh-like”?

Partly misled by the same mistake we made in the fake theorem above, the former researchers restricted their efforts to fit the scatter  $\omega - \psi$  plot of “dipole” by using only one sinh function, which corresponds to two kinds of particles in the “point” theory. In this subsection, it will be seen that we can get a better fitting function if more particles are adopted.

Before making any comparison of two fitting methods, it is necessary to define an indicator of the fitting degree. There are many choices to do that, and the correlation factor is adopted here

$$R^2 = 1 - \frac{\sum_i (\omega_i - f(\psi_i))^2}{\sum_i (\omega_i - \bar{\omega}_i)^2},$$

where  $f$  is the function used to fit the curve, and  $\bar{\omega}_i$  is the space average of  $\omega$ . The larger  $R^2$  is, the better fitting function  $f$  we will obtain (the maximum value of  $R^2$  is 1).

The scatter  $\omega - \psi$  plot to fit is from Fig. 6 of YMC, which is essentially a reproduction of the result of Matthaeus *et al.* [34-36]. As it can be seen in Fig. 10(a), if only two kinds of particles are adopted (the fitting function is limited to one sinh function), there will be some part of the fitting line running away from the scatter plot (indicated by the circle). With four kinds of particles (Fig. 10(b)), a much better fit is obtained. Of course, the more particles are adopted, the better fitting function we will obtain.

Note that in Fig. 10(b), two more unequal strength particles -  $e^{1.07x}$  and  $e^{-1.27x}$  instead of two equal ones (or, another sinh function) are introduced. This is because the asymmetry exists in the  $\omega - \psi$  plot; the unequal strength particles make the fitting better than the sinh functions. Pointin *et al.* use the similar technique in their research before [9], but they also only use two kinds of particles.

For the physical meaning of this fitting process, it is the same problem as the following question:

*How many kinds of vortices are enough to represent the real vorticity field?*

Of course, the more kinds of vortices are adopted, the better.

The discussion above gives out the explanation why sinh-like plots (we know they are not necessary sinh functions anymore) are observed so often in the late time of numerical simulations of 2D decaying turbulence:

In the patch theory, there are millions of  $\omega - \psi$  relations, the general form of which is illustrated in Eq. (6). If sizes of all the patches are shrunk to point, we will always obtain sinh-like plots. Those sinh-like plots do not follow the same formula, but they look the same.

## V. CONCLUSIONS

In this paper, we try to give out a definition of the “final state” of 2D decaying turbulence. Our new definition, which makes use of the effective

area  $S$  in the  $\omega - \psi$  space, is more general than the ordinary functional relation, and can cover all existing results.

We found some new DNS results that can further confirm the predictive power of the statistical mechanics. It is realized that existing numerical results that verify the “patch” theory are those runs starting from narrow-band low wavenumber initial conditions. On the other hand, such less “turbulent” initial conditions tend to lead to “patch” favor results or some weird states that no existing statistical mechanics can explain.

We also found the term “sinh,” which is frequently used in existing literatures of 2D turbulence research, should be replaced by “sinh-like.” It is actually very natural to do that, because the more kinds of particles are used to represent the vorticity field, the more accurate results will be obtained.

Finally, for the integrality of investigations about the “patch” and “point” theory in the statistical mechanics, we should not only connect the statistical theory with numerical simulations (in YMC and this paper), but also connect the theory with experiments:

- For the “patch” theory, so far as to our knowledge, there is no experiment setup that can generate flat vortices, which are illustrated in our numerical simulations. It would be interesting to see such kind of experiments in the future.
- For the “point” theory, it is more easily to generate random point vortices in the laboratory, but our numerical code and theory results are only dealing with double periodical boundary condition for the time being. It is easier to archive high resolutions and perform high Reynolds number simulations by doing this, but it is also difficult to find any experimental comparison. The next step of this research will try to connect the theory with more complex boundaries - for example, the no-slip boundary, which can easily find some laboratory proofs.

## ACKNOWLEDGEMENTS

Numerical simulations in this paper are finished on the SGI Origin 3800 at SARA Supercomputing Center in Amsterdam and the Legend DeepComp 1800 at LSEC, Academy of Mathematics and System Science in Beijing.

I would like to thank Prof. G.J.F van Heijst, Prof. D.C. Montgomery and Dr. H.J.H. Clercx who have contributed to this paper directly or indirectly (make corrections in the corresponding part of my thesis [31]). I also thank

Prof. E. van Groesen, Prof. T.J. Schep, Prof. Annick Pouquet, and Prof. F.W. Sluijter for useful discussions.

I also want to thank D. van der Woude, D. Molenaar, Prof. W. van de Water, W. Kramer, and H. Castelijns, who took part in the “sinh” or “sinh-like” discussion. I thank their efforts to disprove my fake theorem in section IVA, special regard to some of them who tried to prove the fake theorem.

## References

- [1] P.L.Read, P.B. Rhines, and A.A. White, “Geostrophic scatter diagrams and potential vorticity dynamics,” *J. Atmos. Sci.* **43**, 3226 (1986).
- [2] Z. Yin, D. C. Montgomery, and H. J.H. Clercx, “Alternative statistical-mechanical descriptions of decaying two-dimensional turbulence in terms of ‘patches’ and ‘points’,” *Phys. Fluids* **15**, 1937 (2003) (referred to as YMC).
- [3] Z. Yin, H.J.H. Clercx, and D.C. Montgomery, “An easily implemented task-based parallel scheme for the Fourier pseudospectral solver applied to 2D Navier-Stokes turbulence,” *Comput. Fluids* **33**, 509 (2004).
- [4] G.R. Joyce and D. Montgomery, “Negative temperature states for a two-dimensional guiding-centre plasma,” *J. Plasma Phys.* **10**, 107 (1973).
- [5] D. Montgomery and G.R. Joyce, “Statistical mechanics of negative temperature states,” *Phys. Fluids* **17**, 1139 (1974).
- [6] L. Onsager, “Statistical Hydrodynamics,” *Nuovo Cimento Suppl.* **6**, 279 (1949).
- [7] B.E. McDonald, “Numerical calculation of nonunique solutions of a two-dimensional sinh-Poisson equation,” *J. Comp. Phys.* **16**, 630 (1974).
- [8] D.L. Book, S. Fisher, and B.E. McDonald, “Steady-state distributions of interacting discrete vortices,” *Phys. Rev. Lett.* **34**, 4 (1975).
- [9] Y.B. Pointin and T.S. Lundgren, “Statistical mechanics of two-dimensional vortices in a bounded container,” *Phys. Fluids* **19**, 1459 (1976).
- [10] J.H. Williamson, “Statistical mechanics of a guiding-centre plasma,” *J. Plasma Phys.* **17**, 85 (1977).



- [11] A.C. Ting, H.H. Chen, and Y.C. Lee, “Exact solutions of nonlinear boundary value problem: the vortices of the two-dimensional sinh-Poisson equation,” *Physica D* **26**, 37 (1987).
- [12] R.A. Smith, “Phase transition behavior in a negative-temperature guiding-center plasma,” *Phys. Rev. Lett.* **63**, 1479 (1989).
- [13] R.A. Smith and T. O’Neil, “Nonaxisymmetric thermal equilibria of a cylindrically-bounded guiding-center plasma or discrete vortex system,” *Phys. Fluids B* **2**, 2961 (1990).
- [14] R.A. Smith, “Maximization of vortex entropy as an organizing principle of intermittent, decaying, two-dimensional turbulence,” *Phys. Rev. A* **43**, 1126 (1991).
- [15] L.J. Campbell and K. O’Neil, “Statistics of 2-D point vortices and high energy vortex states,” *J. Stat. Phys.* **65**, 495 (1991).
- [16] R. H. Kraichnan and D. Montgomery, “Two-dimensional turbulence,” *Rep. Prog. Phys.* **43**, 547 (1980).
- [17] M. K.-H. Kiessling, “Statistical mechanics of classical particles with logarithmic interactions,” *Comm. Pure Appl. Math.* **46**, 2108 (1993).
- [18] G.L. Eyink and H. Spohn, “Negative temperature states and large-scale, long-lived vortices in two-dimensional turbulence,” *J. Stat. Phys.* **70**, 833 (1993).
- [19] A.J. Chorin, *Vorticity and Turbulence* (Springer, New York, 1994).
- [20] K.W. Chow, N.W.M. Mo, R.C.K. Leung, and S.K. Tang, “Inviscid two dimensional vortex dynamics and a soliton expansion of the sinh-Poisson equation,” *Phys. Fluids* **10**, 1111 (1998).
- [21] B.N. Kuvshinov and T.J. Schep, “Double-periodic arrays of vortices,” *Phys. Fluids* **12**, 3282 (2000).
- [22] F. Spineanu and M. Vlad, “Self-duality of the asymptotic relaxation states of fluids and plasmas,” *Phys. Rev. E* **67**, 046309 (2003).
- [23] K.W. Chow, S.C. Tsang, and C.C. Mak, “Another exact solution for two-dimensional, inviscid sinh Poisson vortex arrays,” *Phys. Fluids* **15**, 2437 (2003).

- [24] R. Robert and J. Sommeria, “Statistical equilibrium states for two-dimensional flow,” *J. Fluid Mech.* **229**, 291 (1991).
- [25] R. Robert and J. Sommeria, “Relaxation towards a statistical equilibrium in two-dimensional perfect fluid dynamics,” *Phys. Rev. Lett.* **69**, 2776 (1992).
- [26] P.H. Chavanis and J. Sommeria, “Classification of self-organized vortices in two-dimensional turbulence: The case of a bounded domain,” *J. Fluid Mech.* **314**, 267 (1996).
- [27] P.H. Chavanis and J. Sommeria, “Classification of robust isolated vortices in two-dimensional hydrodynamics,” *J. Fluid Mech.* **356**, 259 (1998).
- [28] J. Miller, P.C. Weichman, and M.C. Cross, “Statistical Mechanics, Euler’s Equation, and Jupiter’s Red Spot,” *Phys. Rev. A* **45**, 2328 (1992), and references therein.
- [29] H. Brands, S.R. Maassen, and H.J.H. Clercx, “Statistical mechanical predictions and Navier-Stokes dynamics of two-dimensional flows on a bounded domain,” *Phys. Rev. E* **60**, 2864 (1999).
- [30] D. Lynden-Bell, “Statistical mechanics of violent relaxation in stellar systems,” *Mon. Not. R. Astron. Soc.* **136**, 101 (1967).
- [31] Z. Yin, On statistical-mechanical descriptions of decaying two-dimensional turbulence, PhD thesis, Eindhoven University of Technology, The Netherlands (2003).
- [32] E. Segre and S. Kida, “Late states of incompressible 2D decaying vorticity field,” *Fluid Dyn. Res.* **23**, 89 (1998).
- [33] Z.Yin, “Break the bottleneck in the parallelization of 2D spectral Navier-Stokes code,” (in preparation).
- [34] W.H. Matthaeus, W.T. Stribling, D. Martinez, S. Oughton, and D. Montgomery, “Selective decay and coherent vortices in two-dimensional incompressible turbulence,” *Phys. Rev. Lett.* **66**, 2731 (1991).
- [35] W.H. Matthaeus, W.T. Stribling, D. Martinez, S. Oughton, and D. Montgomery, “Decaying two-dimensional turbulence at very long times,” *Physica D* **51**, 531 (1991).

- [36] D. Montgomery, W.H. Matthaeus, W.T. Stribling, D. Martinez, and S. Oughton, “Relaxation in two dimensions and the ‘sinh-Poisson’ equation,” *Phys. Fluids A* **4**, 3 (1992).
- [37] H. Lamb, *Hydrodynamics*, 6th ed. Cambridge University Press, Cambridge (1932).
- [38] J.H.G.M. van Geffen and G.J.F. van Heijst, “Viscous evolution of 2D dipolar vortices,” *Fluid Dyn. Res.* **22**, 191 (1998).
- [39] Such relation, which is also called “the multi-valued function” sometimes, is different from the ordinary definition of the function because the derivatives of it can not be defined. In Eq. (5), the relation we use to derive  $J(\omega, \psi) = 0$  is the normal sense of function, which is so-called one-to-one or many-to-one function (*i.e.* for any value of  $x$ , we can get only one value of  $y$  through relation  $y = f(x)$ ).
- [40] B.M. Boubnov, S.B. Dalziel, and P.F. Linden, “Source-sink turbulence in a stratified fluid,” *J. Fluid Mech.* **261**, 273 (1994).
- [41] Frans de Rooij, P.F. Linden, and Stuart B. Dalziel, “Experimental investigations of quasi-two-dimensional vortices in a stratified fluid with source-sink forcing,” *J. Fluid Mech.* **383**, 249 (1999).

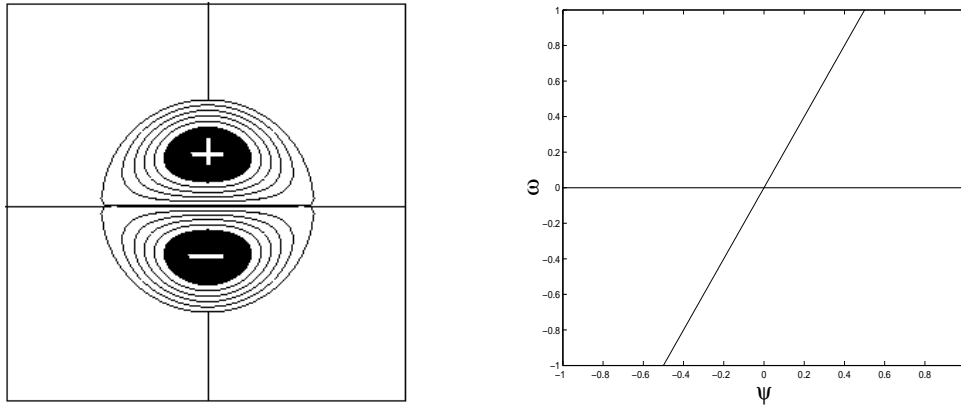


Figure 1: The Lamb dipole with a linear relationship between  $\omega$  and  $\psi$ , can be considered as a stationary two-dimensional solution of the Euler equation. The figure on the left indicates the vorticity field, with one positive vortex and one negative vortex confined within the circle. Outside that circle, the vorticity is zero.

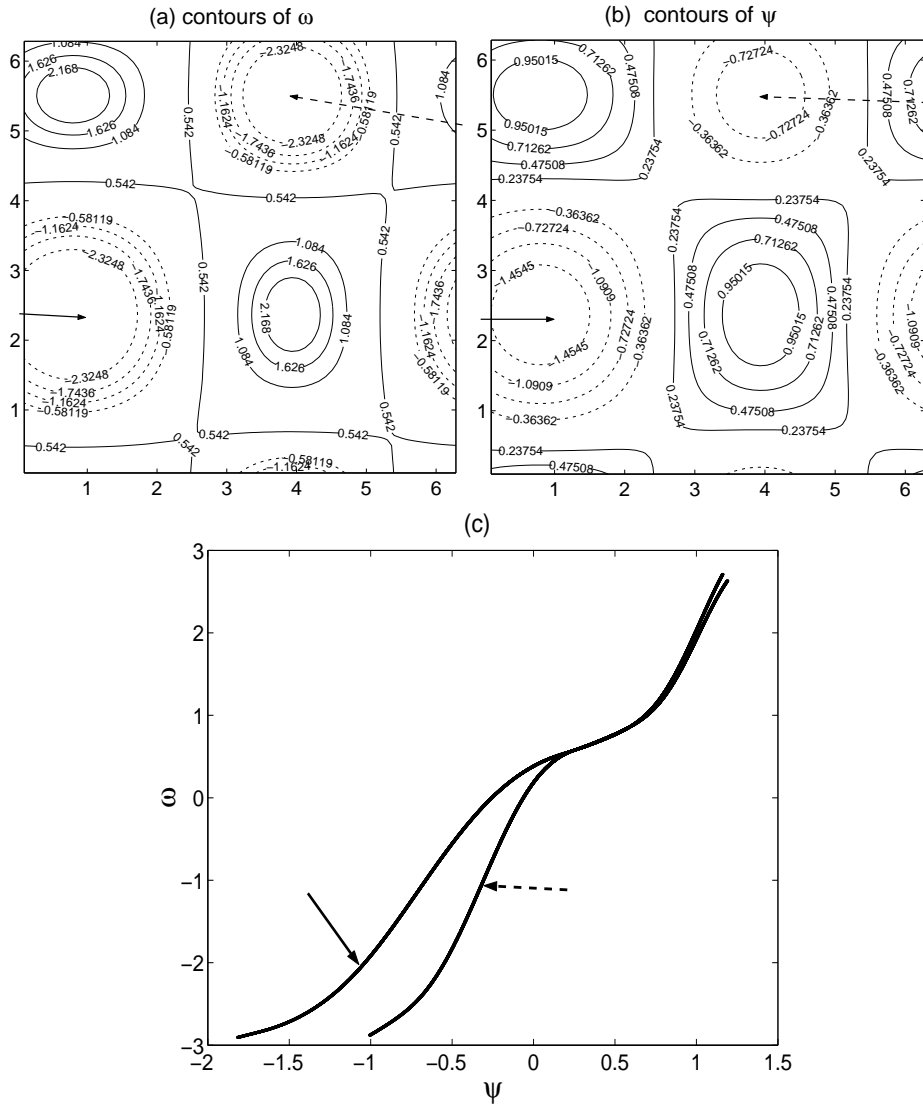


Figure 2: The double-valued structure, representing a non-functional  $\omega - \psi$  relation (c), still is a stationary solution of the Euler equation. The associated vorticity and stream function contour plots are shown in (a) and (b).

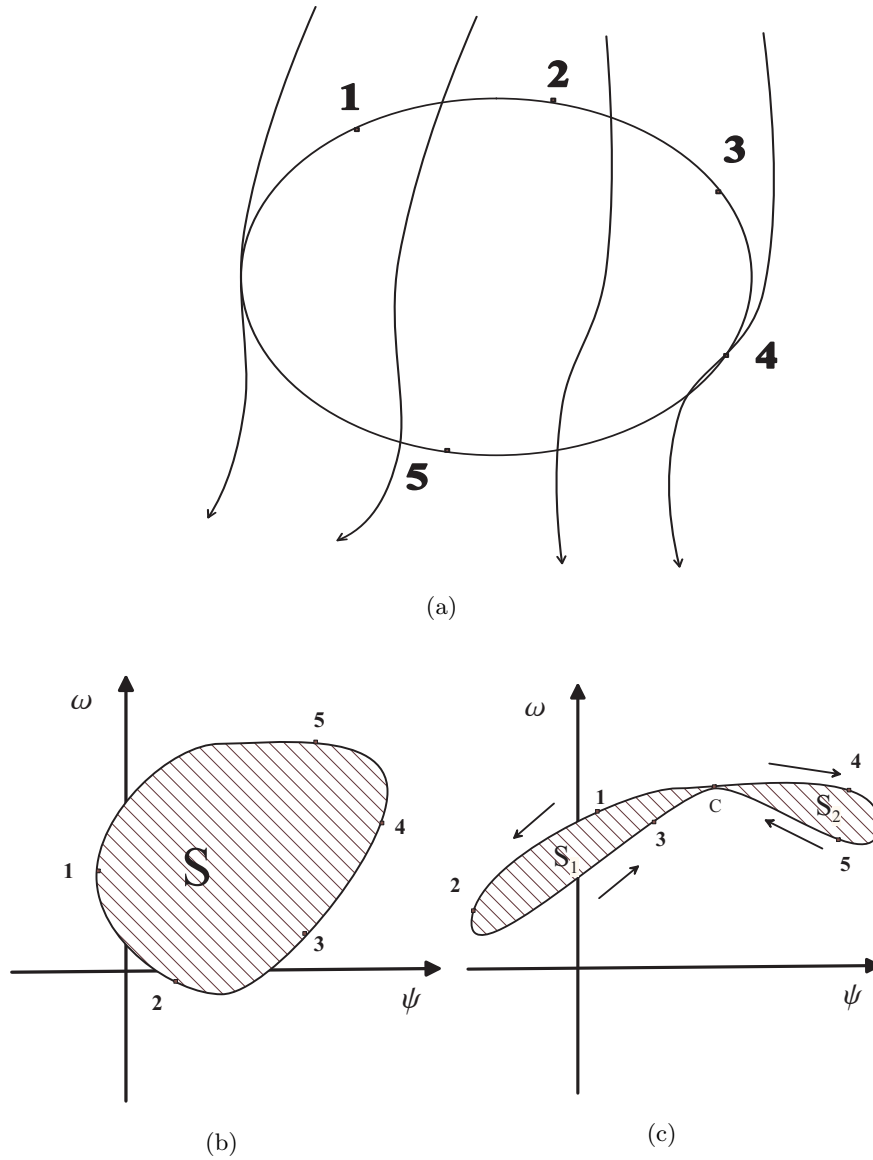


Figure 3: (a) is the contour plot of the stream function  $\psi$  for a flow field, there is a circuit with five marked points on it; (b) indicates one possible distribution of the five marked points in the  $\omega - \psi$  space - they form a simple circuit; (c) indicates another possibility - a reentrant area:  $S_1$  is the anticlockwise region and  $S_2$  the clockwise region.

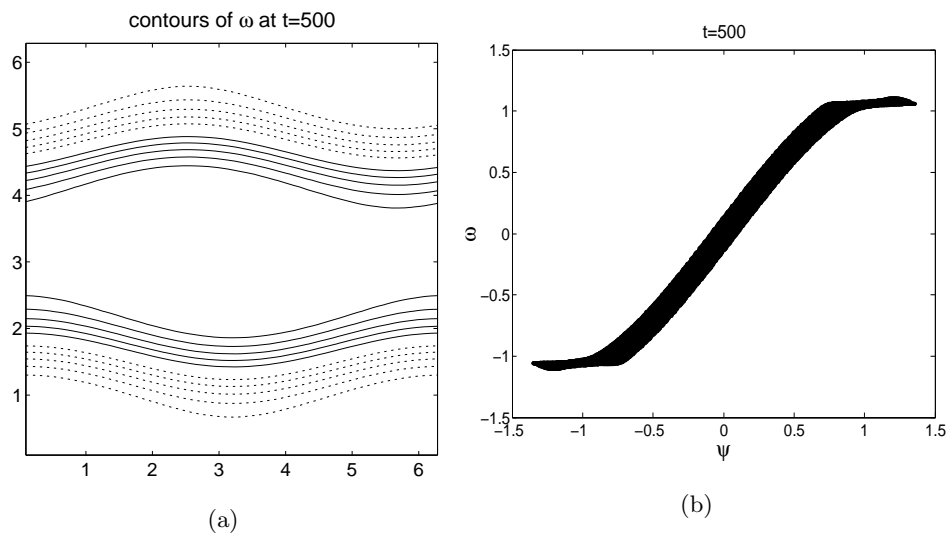


Figure 4: In the late stage of the quadrupole to bar simulation [3], a traveling wave appears and exists for very long time: from  $t = 50$  to  $t = 1000$ . (a) shows one contour plot of the vorticity during this stage; (b) shows the corresponding  $\omega - \psi$  plot. The points in (b) cover a band of area that cannot be treated as zero.

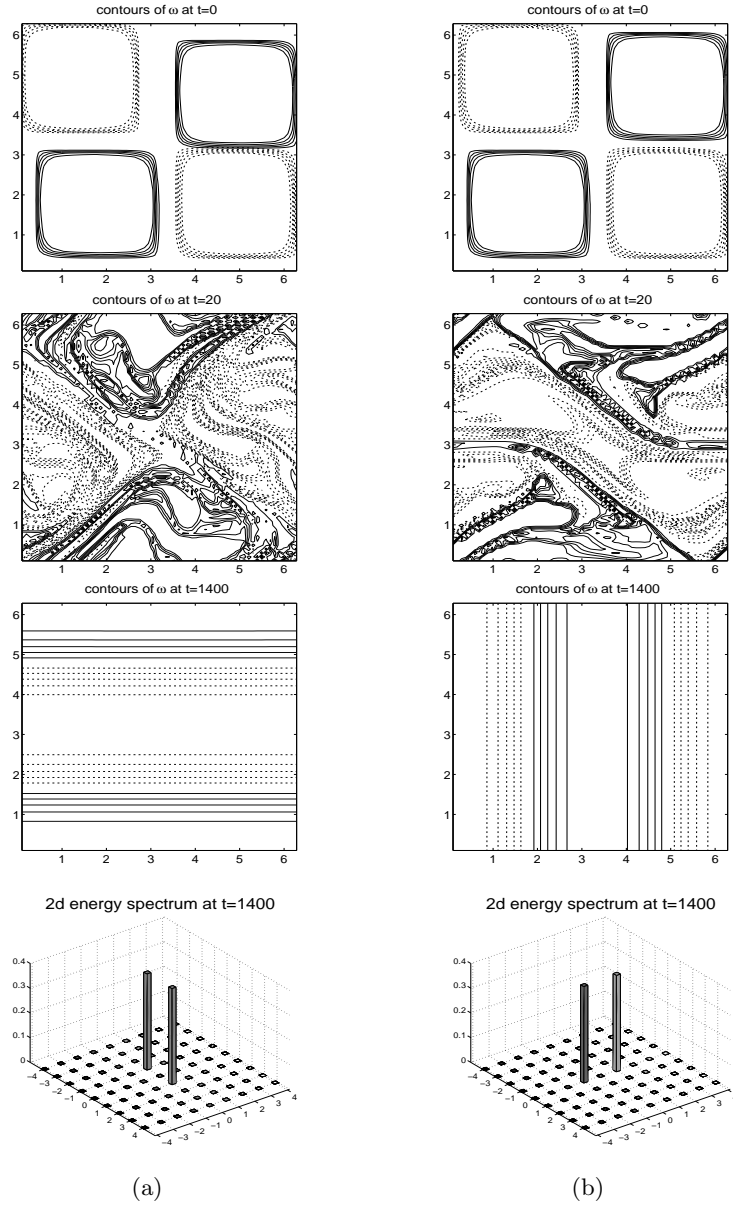


Figure 5: The first three rows are contours of constant vorticity for two runs with slightly different initial conditions in the left (a) and the right (b) column. In both runs, the initial patch sizes are reduced by a factor of  $7/8 \times 7/8 = 49/64$ , and the patches are displaced with respect to the quadrupole initial condition shown in Fig. 7(a) of YMC. Pictures in the fourth row are modal energies of final states at low wavenumbers for two runs.



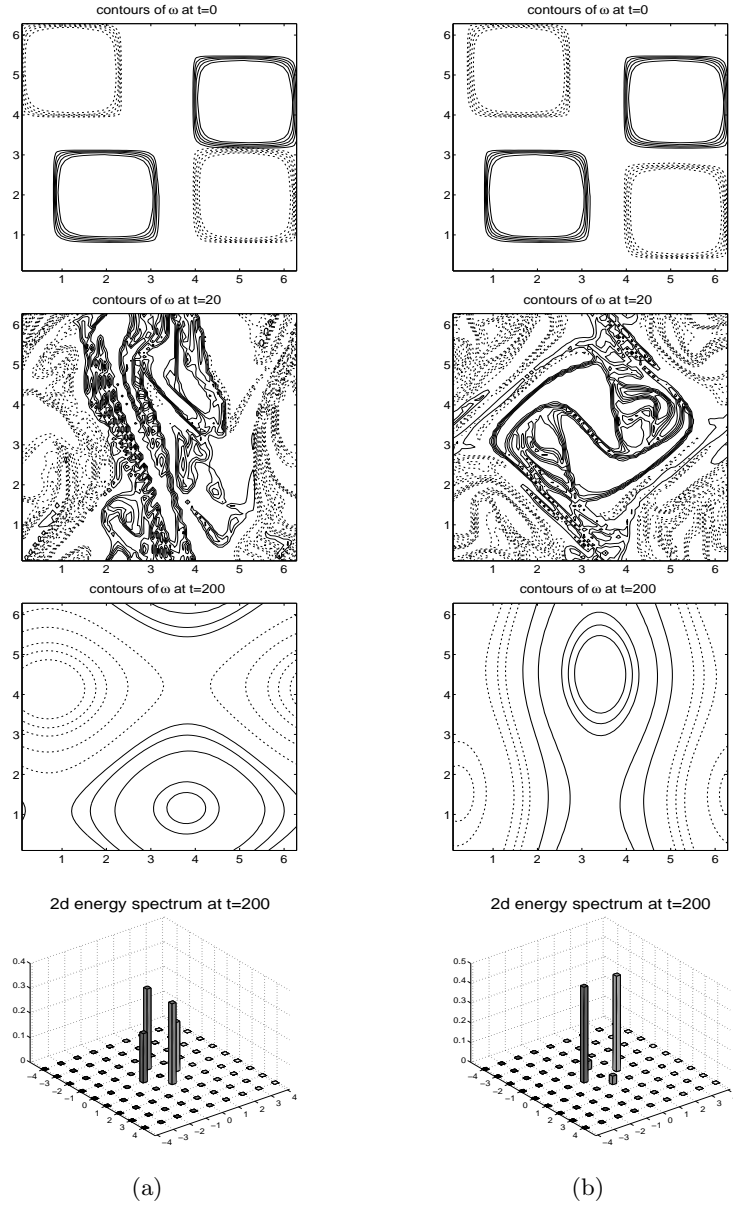


Figure 6: The first three rows are contours of constant vorticity for two runs with slightly different initial conditions in the left (a) and the right (b) column. In both runs, the initial patch sizes are reduced by a factor of  $3/4 \times 3/4 = 9/16$ , which are somewhat larger reductions than initial conditions displayed in Figs. 5, and the patches are displaced with respect to the quadrupole initial condition shown in Fig. 7(a) of YMC. Pictures in the fourth row are modal energies of final states at low wavenumbers for two runs.

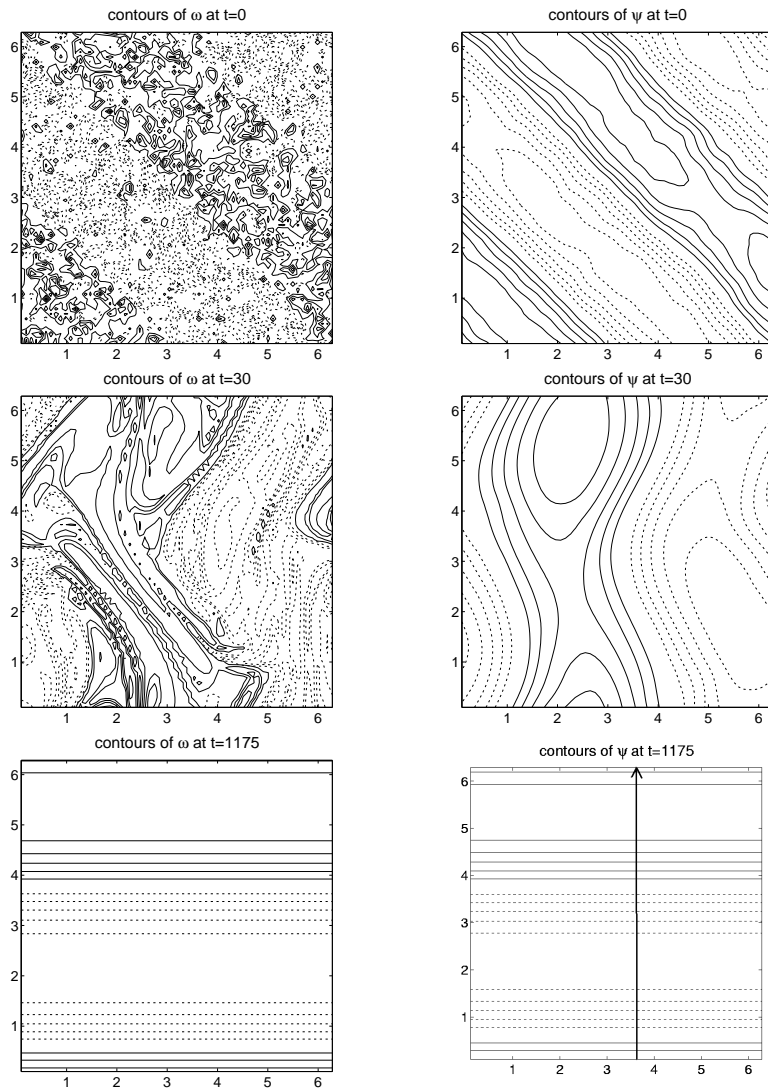


Figure 7: Contours of constant vorticity (left column) and constant stream function (right column) at three different times for the run with a new initial condition leading to the “bar” final state. The arrow line in the last figure of the right column is used to mark the flow field, and calculate the effective area in Fig. 8.

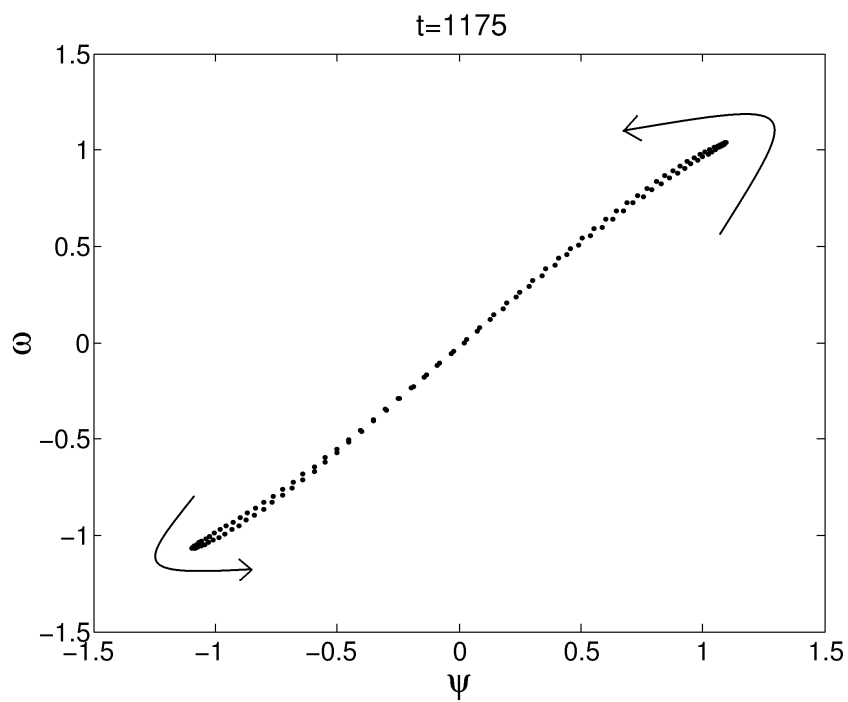


Figure 8: The  $\omega - \psi$  scatter plot for the run shown in Figs. 7. The two ends of the plot are actually two loops. The two arrows indicate the orientations of these two loops, which are obtained by finding the corresponding points along the arrow line in the last plot of Figs. 7.

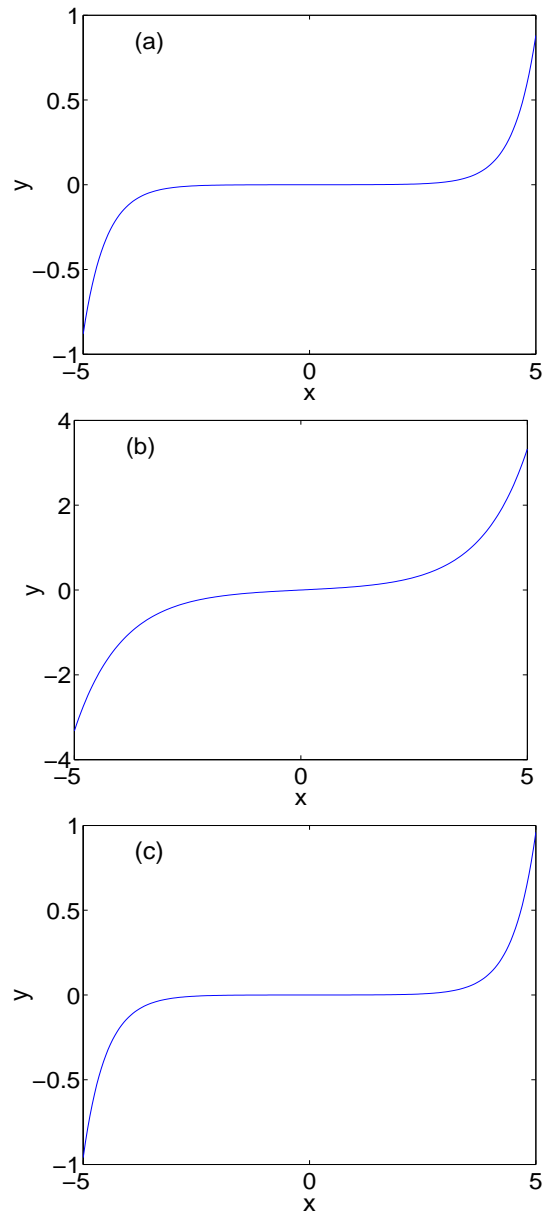


Figure 9: (a) is the plot of one simple sinh function (see Eq. (11)). (b) and (c) are plots of two sums of 100 sinh functions (see Eq. (12) and Eq. (13)); they all look like simple sinh functions.

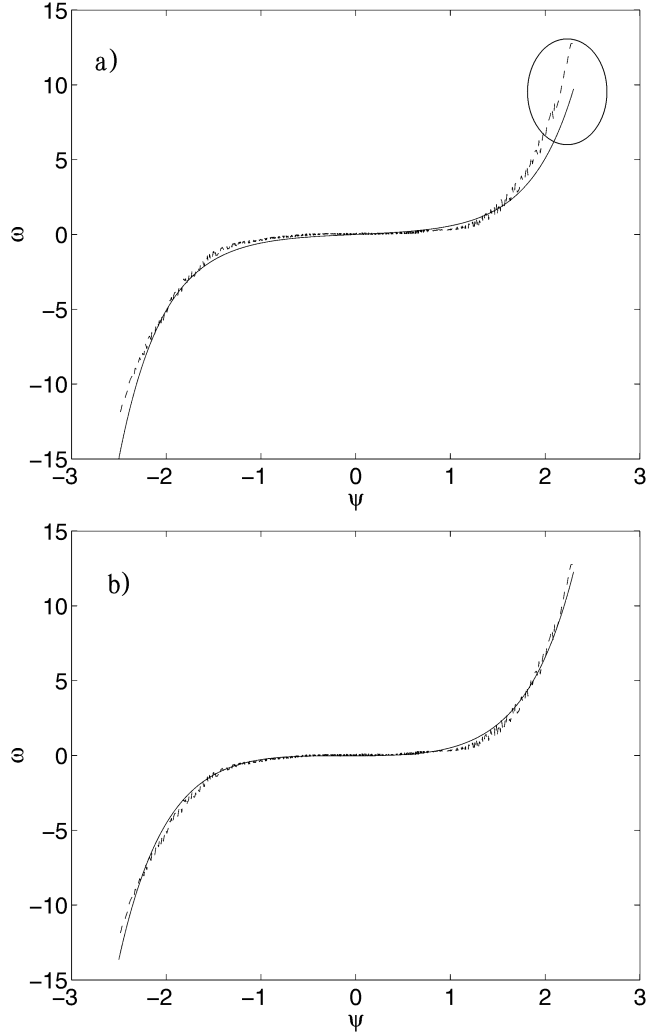


Figure 10: Different functions (indicated by curves drawn through the plotted points) are used to fit the same  $\omega - \psi$  scatter plot of the “dipole” final state. (a) The fitting function is  $y = 0.13\sinh(2.16x)$ , the correlation factor is  $R^2 = 0.95$ . (b) The fitting function is  $y = 0.73\sinh(1.71x) - 0.54e^{1.07x} + 0.52e^{-1.27x}$ , the correlation factor is  $R^2 = 0.99$ .